

## Direct Observation of Millisecond to Second Motions in Proteins by Dipolar CODEX NMR Spectroscopy

Alexey Krushelnitsky,<sup>\*,†</sup> Eduardo deAzevedo,<sup>‡</sup> Rasmus Linser,<sup>§</sup> Bernd Reif,<sup>§</sup> Kay Saalwächter,<sup>\*,||</sup> and Detlef Reichert<sup>\*,||</sup>

Kazan Institute of Biochemistry and Biophysics, Kazan, Russia, Instituto de Física de São Carlos, Universidade de São Paulo, São Carlos, Brazil, Leibniz-Institut für Molekulare Pharmakologie, Berlin, Germany, and Institut für Physik – NMR, Martin-Luther-Universität Halle-Wittenberg, Halle, Germany

Received May 13, 2009; E-mail: krushelnitsky@mail.knc.ru; kay.saalwaechter@physik.uni-halle.de; detlef.reichert@physik.uni-halle.de

The study of protein conformational dynamics is vitally important for the understanding of the molecular mechanisms underlying their biological function.<sup>1</sup> Internal motions on the microsecond to second time scale are of particular interest, since this is the time scale of many biologically relevant events, such as catalysis, recognition, folding, etc. In solution, the exact NMR assessment of such slow motions is challenged by the overall Brownian tumbling that averages dipolar, chemical shift anisotropy (CSA), and quadrupolar interactions. In contrast, in the solid state, these interactions can be beneficially employed to access the whole frequency range of internal protein dynamics, along with a direct elucidation of the geometric details of molecular motions. Studies of site-resolved internal dynamics in solid proteins to date have been limited to nanosecond to microsecond time scales.<sup>2–5</sup> For slower dynamics, there is still a considerable lack of experimental tools that can provide reliable quantitative information.

In this communication, we demonstrate for the first time a site-resolved study of slow (ms to s) motions in a microcrystalline protein, namely, the SH3 domain of  $\alpha$ -spectrin. We apply an improved variant of a well-known solid-state magic-angle-spinning (MAS) exchange experiment, centerband-only detection of exchange (CODEX),<sup>6</sup> which yields direct time-domain dynamic information. CODEX was originally based on measuring changes in molecular orientation by means of changes in the CSA tensor orientation, which is encoded under MAS conditions by means of recoupling of  $\pi$  pulses in a way analogous to that in the well-known dipolar-recoupling rotational-echo double-resonance (REDOR) experiment.<sup>7</sup> CSA-based CODEX has previously been applied to the study of biomolecular dynamics,<sup>6c</sup> but it is subject to limitations that we improve upon herein.

We make use of the basic principle of CODEX, yet we employ heteronuclear dipolar couplings instead of CSA, which offers crucial advantages. In general terms, CODEX starts with an encoding during a time period A that under REDOR-type recoupling yields an accumulated phase  $\phi_A$ . Magnetization is then stored along  $z$  during a mixing time  $\tau_m$ , where molecular reorientation can occur. After  $\tau_m$ , the magnetization is allowed to evolve during a period B under identical recoupling conditions, during which it accumulates a phase  $\phi_B$ . When the pulse phases are properly set, the amplitude of the signal obtained after a readout period (another  $z$  storage followed by a readout pulse) is proportional to

$$I \sim \langle \cos \phi_A \cos \phi_B \rangle + \langle \sin \phi_A \sin \phi_B \rangle = \langle \cos(\phi_A - \phi_B) \rangle$$

where the brackets denote a powder average. If no change of molecular orientation occurs during  $\tau_m$ , then  $\phi_A = \phi_B$  and a full echo ( $I_0 = 1$ ) is measured. If the tensor orientation is modulated by molecular motion, then  $\phi_A \neq \phi_B$  and the signal intensity decreases. In the limit of long mixing and encoding times, the normalized intensity  $I/I_0 = f_\infty = 1/N$  can be directly interpreted in terms of the number of sites  $N$  accessible to the process. The time scale of the original CODEX method is limited to the millisecond range at the lower end by the recoupling time itself,<sup>8</sup> and the upper limit in the second range is set by  $T_1$  processes, (proton-driven) spin diffusion,<sup>9</sup> and  $T_1$  relaxation processes of other nuclei (the relaxation-induced dipolar exchange with recoupling (RIDER) effect).<sup>10</sup>

Proton-driven spin diffusion among  $^{15}\text{N}$  (not to mention  $^{13}\text{C}$ ) nuclei in fully enriched protonated proteins is in fact the major challenge for studying dynamics by means of solid-state exchange NMR, prompting us to apply CODEX to deuterated (proton-depleted) samples that were partially back-exchanged at labile sites.<sup>11</sup> Proton dilution provides not only suppression of spin diffusion but also a significant sensitivity enhancement in the case of indirect proton detection with high signal-to-noise ratio. Furthermore, the use of heteronuclear dipolar interactions instead of CSA is advantageous because XH dipolar tensors are usually larger than the CSA and have axial symmetry and orientations that are well-known from the structure. For this purpose, the REDOR train of  $\pi$  pulses is applied on the H channel (see Figure 1). The single

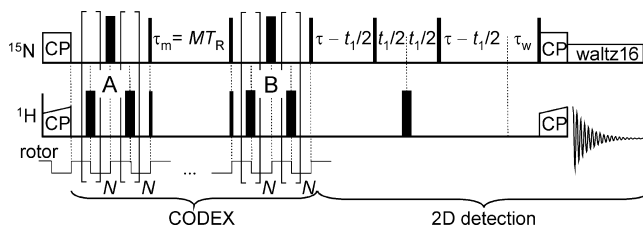


**Figure 1.** Dipolar CODEX pulse sequence. Thin and thick sticks denote  $\pi/2$  and  $\pi$  pulses, respectively, and  $\tau_w$  is a delay for better cancellation of the residual water signal.

X-channel  $\pi$  pulse in the middle of the encoding periods serves to remove the influence of isotropic chemical shifts. There must be an integer number of rotor periods before and after this  $\pi$  pulse; otherwise, part of the  $^{15}\text{N}$  CSA and  $^2\text{H}$ – $^{15}\text{N}$  dipolar interactions would be reintroduced. Thus, the number of the rotor periods in the time intervals A and B must be an even number, and  $N$  (the number of  $^1\text{H}$   $\pi$  pulses within half of the periods A and B; see Figure 1) must be an odd number.

<sup>†</sup> Kazan Institute of Biochemistry and Biophysics.

<sup>‡</sup> Universidade de São Paulo.

<sup>§</sup> Leibniz-Institut für Molekulare Pharmakologie.

<sup>||</sup> Martin-Luther-Universität Halle-Wittenberg.

For dipolar CODEX, the cos and sin components are related not just to the  $x$  and  $y$  components of the transverse X magnetization but to in-phase  $S_x$  and antiphase  $2S_yI_z$  terms, respectively. As the most crucial advantage, couplings to other NMR-active nuclei, e.g., deuterons, are not reintroduced and thus do not pose problems related to their respective  $T_1$  relaxation (RIDER). The unavoidable recoupling of dipolar interactions to other heteronuclei is one of the most serious limitations of the original CSA-based CODEX experiment.<sup>10</sup>

The antiphase term can create problems, as the  $I_z$  component is destroyed by spin exchange (actual exchange or spin diffusion) as well as faster  $T_1$  relaxation.<sup>10</sup> In our sample, the  $^1\text{H}$   $T_1$  was  $\sim 1.6$  s, which would be a serious limitation. To avoid this, we reduced the original phase cycle so only the  $\langle \cos \phi_A \cos \phi_B \rangle$  component related to in-phase magnetization was measured. This did not challenge the sensitivity of the experiment at all, as the sin counterpart would in any event be measured in separate transients as part of a longer phase cycle.<sup>6</sup> The experiment is thus largely similar to established stimulated-echo experiments that are very common in NMR analysis of static samples.<sup>12</sup> Notably, the sensitivity is reduced for passive spins with  $I > 1/2$  and for  $\text{XH}_n$  groups, for which the maximum amplitude of the cos-cos term is smaller.

We applied the experiment to  $^{15}\text{N}$ - $^1\text{H}$  dipolar pairs, but it can of course be applied to any other pair of magnetic nuclei. The pulse sequence in Figure 1 shows the combination of the dipolar CODEX part with a proton-detected  $^{15}\text{N}$ - $^1\text{H}$  2D correlation experiment.<sup>11</sup> The use of a proton-depleted sample also provides longer effective  $T_2$  relaxation times<sup>13</sup> (up to 100 ms) during the encoding delays and thus a better signal. By virtue of the restriction to encoding  $S_x$  in-phase magnetization, the experiment is not affected at all by fast interproton spin diffusion or relaxation, even in fully protonated samples. Proton-driven  $^{15}\text{N}$ - $^{15}\text{N}$  spin diffusion can also be ruled out, as previous work has demonstrated a spin-diffusion time scale of  $\sim 5$  s in a fully protonated protein at 10 kHz MAS,<sup>14</sup> so the additional slowdown in the deuterated protein provides enough headspace.

An important experimental detail is the correction of the experimental CODEX exchange intensities (measured as a function of the mixing time  $\tau_m$ ) for  $T_1$  relaxation of the observed  $^{15}\text{N}$  nucleus. The original CODEX pulse sequence implements an internal  $T_1$  normalization by means of referencing (dividing) the signal by that of a largely identical reference experiment with swapped mixing and  $z$ -filter delays.<sup>6</sup> This approach is elegant but has two drawbacks: first, the signal-to-noise ratio suffers as a result of the division by another noisy quantity, and second, the reference experiment sacrifices half of the spectral intensity because of separate  $z$ -storage of the cos and sin components during  $\tau_m$ . We therefore correct for  $T_1$  effects via a conventional separate measurement (as described in ref 5) and subsequent division of the exchange intensities by a (noiseless) spin-lattice relaxation decay function, as we did in our previous papers.<sup>9,14</sup>

Since there are also no losses due to  $T_2$  relaxation, the  $T_1$  measurements are  $\sim 4$  times faster than the CODEX measurements, and the experimental uncertainties in the  $T_1$  values (3–15%) do not challenge the results reported below. Most of the peaks showed single-exponential decays, but there were a few peaks that revealed double-exponential  $T_1$  decays, which can be explained by (partial) overlap of signals, an example of which is discussed below. It should be noted that  $T_1$  values that are comparable to the range of mixing times used in the CODEX experiment compromise the signal intensity at long mixing times, leading to larger error intervals at longer  $\tau_m$  but not to large systematic errors. Details of the  $T_1$  correction of the CODEX decays are illustrated in Figures S2 and S3 in the Supporting Information (SI).

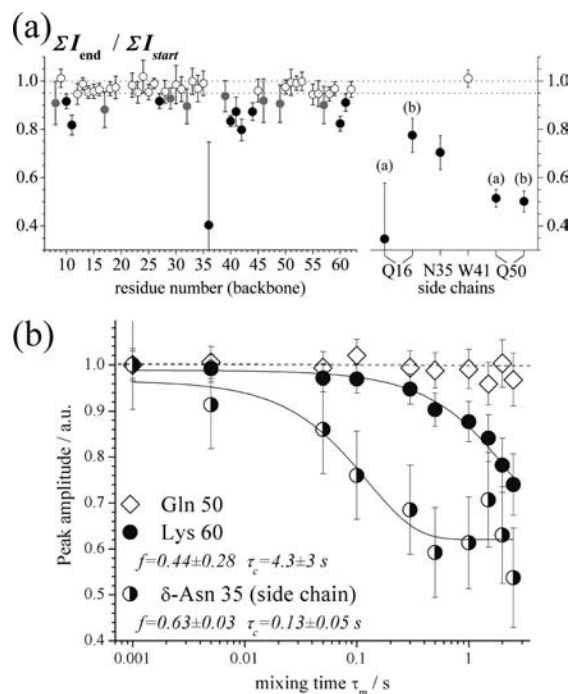


**Figure 2.** (a) Residue-resolved ratios of exchange intensities (corrected for spin-lattice relaxation) taken at the end (the last four points) and at the beginning (the first four points) of the CODEX decay, identifying residues with mobility on a ms-to-s scale. Solid circles define  $\Sigma I_{\text{end}}/\Sigma I_{\text{start}}$  ratios with the upper limit of the error margin below 0.95. Gray circles define the ratios less than 0.95 for which the error margin exceeds the value of 0.95. (b) Examples of  $\tau_m$  dependences for residues undergoing (Lys 60 and  $\delta$ -Asn 35) and not undergoing (Gln 50) slow motions. The lines are exponential fits. Experimental conditions: Bruker Avance III 600 MHz spectrometer, narrow-bore 4 mm MAS probe, 10 kHz MAS at 14 °C, 0.8 ms encoding periods ( $N = 7$ ; see Figure 1).

In Figure 2, we demonstrate the potential of the technique as applied to slow conformational motions in the SH3 domain of  $\alpha$ -spectrin, which was perdeuterated with 20% back-substitution of labile protons. Ten mixing times between 1 ms and 2.5 s were recorded. To present the results of the analysis of the exchange decays for all of the peaks in one figure, we have plotted the ratio of the sum of the intensities of the last four points (1–2.5 s) of the decay to the sum of the intensities of the first four points (1 ms–0.1 s) of the same decay (see Figures S4 and S5 in the SI). This ratio provides a measure of the amplitude of the exchange decay with a relatively small experimental error and thus indicates residues undergoing slow motions. To identify signals undergoing exchange with appreciable amplitude beyond the experimental error, we have marked as black circles all the points in Figure 2a having an upper limit of the error margin less than 0.95. In addition, the remaining points in Figure 2a having an exchange ratio less than 0.95, regardless of their error, are marked in gray. The decays of all the marked peaks are shown in the SI. Thus, it is seen that about half the residues undergo slow motions. The large number of residues involved in slow motions is in fact expected, since infrequent large-scale conformational jumps in densely packed native proteins by default require correlated rearrangements of larger structural units. The color-coded presentation of mobile residues in the protein structure presented in Figure 3 shows that most of the residues undergoing slow motion are located at the termini and in a stretch in the center of the polypeptide chain from S36 to R49. It is important to mention that not only loops but also secondary-structure elements are involved in the slow motion.

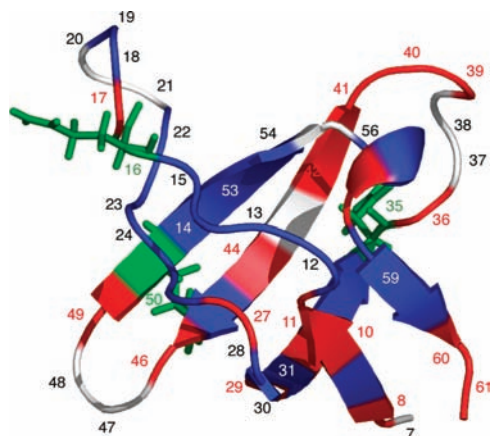


**Figure 3.** Structure of the  $\alpha$ -spectrin SH3 domain with color-coded residue mobility: blue indicates immobile residues, and red (backbone) and green (side chains) indicate mobile residues (black and gray circles in Figure 2a). Residues that are unassigned or not seen in the spectrum are white.

Fitting of the decays with a single-exponential function,  $I(\tau_m) \sim (1-f) \exp(-\tau_m/\tau_c) + f$  (see Figures 2b and S4) demonstrates that almost all the indicated residues feature correlation times of 1–3 s. Thus, it is likely that there is one dominant mode of slow motion in the protein involving a range of residues located in different parts of the spatial structure. There are only three exceptions that exhibit appreciably shorter correlation times: backbone peak Ser 36 and side-chain peaks Gln 16(b) and Asn 35 (see Figure S4 in the SI). However, Ser 36 has the largest experimental error of all the peaks, and thus, the fit of this decay is not very reliable. The fit of Gln 16(b) is problematic (see below), so the side chain of Asn 35 seems to be the only protein fragment undergoing another mode of slow motion independent of the rest of the molecule. However, this does not seem unreasonable for a separated side chain located on the protein surface.

It should be noted that the final plateau value  $f_\infty$  obtained at long mixing and encoding times might well be even lower than the plateau value that we observed in some cases, precluding for the moment the elucidation of geometric details of the motions, such as jump angles. Such work is time-consuming, as it requires checking the dependence on the recoupling time given in  $N + 1$  rotor cycles (see Figure 1). Another challenge is that a potential preaveraging of the  $^{15}\text{N}$ – $^1\text{H}$  dipolar couplings resulting from faster motions on the picosecond to microsecond time scale must be quantified before the geometry can be addressed in any detail. Such investigations, using DIPSHIFT<sup>15a</sup> and Lee–Goldburg CP experiments,<sup>15b</sup> are underway. However, the fact that under the given conditions we have already observed long-time intensity values significantly less than 0.5 (and even values close to 0 for the side-chain signals) indicates that the corresponding residues undergo multisite jumps. We emphasize that the extracted correlation times are independent of the observed plateau values  $f$  and thus independent of the geometry of motion, at least in homogeneous systems without large-scale disorder, as is the case for our microcrystalline protein.

It is interesting to note that with only one exception (Trp 41), all the assigned side-chain signals (Gln 16, Asn 35, and Gln50) undergo slow motion. The exchange decays of the two side-chain nitrogens of  $\epsilon$ -Gln 50 with  $f \approx 0.2$  and  $\tau_c \approx 1.7$  s are similar, as they should be, since conformational jumps experienced by this side chain must be equally reflected in the motion of two N–H bonds. The difference in the values of the  $f$  parameter for these two peaks (0.1 vs 0.3) is explained by the fact that the maximum mixing time used in the experiment was not long enough to reach the true plateau, resulting in a larger error in this parameter and a

smaller systematic error in the correlation times (using longer mixing times would be of little help because of the relatively short  $T_1$  of these peaks). At the same time, the  $\tau_c$  of the two Gln 16 peaks (0.35 vs 2.5 s) are appreciably different, and this difference cannot be explained by uncertainty in the fits. The reason is the substantial overlap of the second peak (b) of  $\epsilon$ -Gln 16 with another peak, namely, Val 23 of the backbone (see Figure S1 in the SI), which we did not attempt to deconvolute. The (static) contribution from Val 23 produces artificially high intensities at longer mixing times, leading to an apparently higher plateau and an unreliable fit. It should be noted that the  $T_1$  correction fails in cases where the  $T_1$ 's of superposed signals differ appreciably.

In summary, we have demonstrated the use a new dipolar exchange experiment for high-resolution biomolecular solid-state NMR spectroscopy that provides unique and as yet inaccessible *direct* (i.e., truly model-free) information on time scales and geometry of millisecond to second dynamics, paving the way for future applications in studies of actual protein function. In general, the presented data is free from interfering magnetic effects such as spin diffusion, RIDER, and  $T_1$  relaxation, the latter only indirectly limiting the sensitivity of the method to measuring correlation times on the order of the  $^{15}\text{N}$   $T_1$ . Notably, observing slow motions on a second time scale in the liquid state by means of  $R_2/R_{1\rho}$  dispersions<sup>16</sup> is problematic if not impossible. It is intriguing that even small, rigid globular proteins, such as the SH3 domain, show a rich variety of slow motions. Relating these motions to the dynamics of the protein in its native state (solution) is highly worthwhile, possibly elucidating internal constraints versus crystalline packing, and is a goal of future work.

**Acknowledgment.** This work was supported by the European Union (ERDF), the Fonds der Chemischen Industrie, and a grant from the Program “Molecular and Cell Biology” of the Russian Academy of Sciences. We thank V. Chevelkov and C. Hackel for their assistance in the experiments and data analysis.

**Supporting Information Available:** 2D spectrum with assignments, details of the  $T_1$  correction of the CODEX decays, and examples of the CODEX mixing-time dependences for various peaks. This material is available free of charge via the Internet at <http://pubs.acs.org>.

## References

- (1) (a) Wand, A. *J. Nat. Struct. Biol.* **2001**, *8*, 926. (b) Karplus, M.; Kuriyan, J. *Proc. Natl. Acad. Sci. U.S.A.* **2005**, *102*, 6679.
- (2) Giraud, N.; Bockmann, A.; Lesage, A.; Penin, F.; Blackledge, M.; Emsley, L. *J. Am. Chem. Soc.* **2004**, *126*, 11422.
- (3) Hologne, M.; Faelber, K.; Diehl, A.; Reif, B. *J. Am. Chem. Soc.* **2005**, *127*, 11208.
- (4) Lorieau, J. L.; McDermott, A. E. *J. Am. Chem. Soc.* **2006**, *128*, 11505.
- (5) Chevelkov, V.; Diehl, A.; Reif, B. *J. Chem. Phys.* **2008**, *128*, 052316.
- (6) (a) deAzevedo, E. R.; Hu, W.-G.; Bonagamba, T. J.; Schmidt-Rohr, K. *J. Am. Chem. Soc.* **1999**, *121*, 8411. (b) deAzevedo, E. R.; Hu, W.-G.; Bonagamba, T. J.; Schmidt-Rohr, K. *J. Chem. Phys.* **2000**, *112*, 8988. (c) deAzevedo, E. R.; Kennedy, S. B.; Hong, M. *Chem. Phys. Lett.* **2000**, *321*, 43.
- (7) Gullion, T.; Schaefer, J. *J. Magn. Reson.* **1989**, *81*, 196.
- (8) Saalwächter, K.; Fischbach, I. *J. Magn. Reson.* **2002**, *157*, 17.
- (9) Krushelnitsky, A.; Reichert, D.; Hempel, G.; Fedotov, V.; Schneider, H.; Yagodina, L.; Schulga, A. *J. Magn. Reson.* **1999**, *138*, 244.
- (10) Saalwächter, K.; Schmidt-Rohr, K. *J. Magn. Reson.* **2000**, *145*, 161.
- (11) Chevelkov, V.; Rehbein, K.; Diehl, A.; Reif, B. *Angew. Chem., Int. Ed.* **2006**, *45*, 3878.
- (12) Böhrer, R.; Diezemann, G.; Hinze, G.; Rössler, E. *Prog. NMR Spectrosc.* **2001**, *39*, 191.
- (13) Chevelkov, V.; Reif, B. *Concepts Magn. Reson.* **2008**, *32A*, 143.
- (14) Krushelnitsky, A.; Bräuniger, T.; Reichert, D. *J. Magn. Reson.* **2006**, *182*, 339.
- (15) (a) deAzevedo, E. R.; Saalwächter, K.; Pascui, O.; de Souza, A. A.; Bonagamba, T. J.; Reichert, D. *J. Chem. Phys.* **2008**, *122*, 104505. (b) Cobo, M. F.; Maliňáková, K.; Reichert, D.; Saalwächter, K.; deAzevedo, E. R. *Phys. Chem. Chem. Phys.* **2009**, *11*, 7036.
- (16) Palmer, A. G.; Kroenke, C. D.; Loria, J. P. *Methods Enzymol.* **2001**, *339*, 204.

JA9038888